

Supporting Information

Oxygen Activation at a Dicobalt Center of a Dipyridylethane Naphthyridine Complex

Casey N. Brodsky,^a Guillaume Passard,^a Andrew M. Ullman,^a David E. Jaramillo,^a
Eric Bloch,^{a,b} Michael Huynh,^a David Gygi,^a Cyrille Costentin^{a,c} and Daniel G. Nocera^{a,*}

^a *Department of Chemistry and Chemical Biology, Harvard University, Cambridge, Massachusetts
02138, United States. E-mail: dnocera@fas.harvard.edu*

^b *Present Address: Department of Chemistry and Biochemistry, University of Delaware, Newark, Dela-
ware 19716, United States. E-mail: edb@udel.edu*

^c *Laboratoire d'Electrochimie Moléculaire, Unité Mixte de Recherche Université - CNRS N° 7591, Bâti-
ment Lavoisier, Université Paris Diderot, Sorbonne Paris Cité, 15 rue Jean de Baïf, 75205 Paris Cedex
13, France. E-mail: cyrille.costentin@univ-paris-diderot.fr*

<i>Table of Contents</i>	<i>Page</i>
A. Experimental Methods	S3
A.1. Electrochemistry	S3
A.2. Synthesis	S3
A.3. Characterization methods	S6
A.4. X-ray crystallography	S6
A.5. Details for fitting VT ¹ H NMR	S7
A.6. Computational details	S8
B. Figures	S9
Figure S1. ¹ H NMR of compounds 1 , 2 and 3	S9
Figure S2. Scan rate dependence CV and DOSY NMR of compound 1	S10
Figure S3. Simulation of E(EC) mechanism	S11
Figure S4. ¹ H NMR monitoring of O ₂ binding to compound 2	S12
Figure S5. XPS of compounds 1 , 2 , and 3	S13
Figure S6. Absorption spectrum of 3 obtained from reaction of 1 with UHP	S14
Figure S7. CV of 3 in presence of acid and comparison to 1 under ORR	S15
Figure S8. DFT of proposed peroxide, compound 3	S16
References	S17

A. Experimental Methods

A.1. Electrochemistry

Cyclic voltammograms (CVs) were recorded using a CH Instruments potentiostat. Compounds were dissolved in a given organic solvent (previously purified and dried by passing through a neutral alumina column under argon) containing supporting electrolyte, 0.1 M *n*-Bu₄NPF₆ (purchased from Sigma Aldrich, used without any purification and stored under vacuum). A three-electrode cell configuration was used where the counter electrode was a platinum wire, the reference electrode was a saturated calomel electrode (SCE) separated from the solution by a frit containing a solution of supporting electrolyte, and the working electrode was a glassy carbon button electrode (diameter 3mm) that was carefully polished before each measurement. The polishing procedure was performed for 2 min on felt using different diamond pastes subsequently of 15, 6, 3 and 1 μm. Ethanol was used as a lubricant and to remove the diamond paste from the electrode. Before using the electrode, it was briefly sonicated in ethanol and dried with a stream of compressed air. Between each recorded CV, the polishing procedure was repeated using 1 μm paste. The ohmic drop was carefully compensated in all electrochemical experiments by using the positive feedback compensation implemented in the instrument.

Bulk electrolysis was performed using a CH Instruments potentiostat. The experiments were performed in a cell with a carbon crucible as working electrode ($S = 20 \text{ cm}^2$); the volume of the solution was 10 mL. The reference electrode was an aqueous SCE electrode and the counter electrode a platinum mesh in a bridge separated from the cathodic compartment by a glass frit, containing a 0.4 M [Et₄N⁺][CH₃CO₂⁻] and supporting electrolyte solution. The role of [Et₄N⁺][CH₃CO₂⁻] was to serve as reactant at the anode, producing CO₂ and ethane (Kolbe reaction). The electrolysis solution was purged with Ar for few minutes prior electrolysis. The reference electrode was directly immersed in the solution (without separated bridge) and situated progressively closer to the working electrode to minimize the ohmic drop.

Thin-layer UV-vis spectroelectrochemistry experiments were performed using a 0.5 mm path length quartz cell with an Ocean Optics USB4000 spectrophotometer and DT-Mini- 2GS UV-vis-nIR light source in conjunction with the CH electrochemical workstation described above. Samples were prepared as 1 mM of compound **1** plus 1.5 mM TFA in 0.1 M *n*-Bu₄NPF₆ in MeCN. Bulk electrolysis was performed using a Pt flag working electrode, a Ag wire reference electrode, and a Pt wire counter electrode.

A.2. Synthesis

Preparation of dipyridylethane naphthyridine (DPEN). Two literature methods [1,2] were combined in the following adaptation. *n*-Butyllithium (2.5 M in hexanes, 14.0 mL, 35.0 mmol, 4.60 equiv) was added dropwise to a stirring solution of 2-ethylpyridine (4.67 mL, 40.8 mmol, 5.37 equiv) in 100 mL of THF at -78 °C. The resulting deep red solution was

stirred at $-78\text{ }^{\circ}\text{C}$ for 30 min. The flask was then removed from the cooling bath, and 2-fluoropyridine (1.51 mL, 17.5 mmol, 2.30 equiv) was immediately added dropwise. The mixture was stirred for 1 h as it slowly warmed to room temperature, and then it was placed in an oil bath to reflux for 1 h under an atmosphere of N_2 . The flask was then removed from the oil bath and cooled to room temperature over 30 min. Under positive N_2 pressure, solid 2,7-dichloro-1,8-naphthyridine (1.51 g, 7.59 mmol, 1.00 equiv) was added to the stirring mixture, and the flask was returned to the oil bath to reflux for 16 h under an atmosphere of N_2 . After cooling to room temperature, the reaction mixture was quenched with 100 mL of water, concentrated to remove the majority of the THF, and extracted with $3 \times 200\text{ mL}$ of CH_2Cl_2 . Organics were combined, dried over MgSO_4 , filtered, and concentrated. The residual material was recrystallized from 200 mL of hot MeCN to give 2.84 g of DPEN. The filtrate from the first crystallization was concentrated and redissolved in 100 mL of hot MeCN to yield a second batch (0.39 g) of crystals of DPEN. Total yield of 3.24 g, 6.55 mmol, 86.3%. Characterization data for this material (^1H NMR, ESI-MS) were in accordance with the literature [1].

Preparation of $[\text{Co}_2(\text{OH})_2\text{DPEN}(\mu\text{-}1,3\text{-OC}(\text{NH})\text{CH}_3)](\text{PF}_6)_3$ (1**).** $\text{Co}(\text{NO}_3)_2$ (0.2 M aq solution, 14.2 mL, 2.84 mmol) was added to a solution of DPEN (702 mg, 1.42 mmol) in 5 mL of acetone. After stirring at room temperature for 20 min, H_2O_2 (9.79 M aq solution, 290 μL , 2.84 mmol) was added, and the reaction mixture was stirred for 16 h at room temperature. The mixture was then concentrated at $60\text{ }^{\circ}\text{C}$ to a volume of 3 mL to which one drop of 10% HNO_3 was added and 50 mL of acetone was quickly added to the concentrate, resulting in the precipitation of a pink solid. The solid was collected on 5 μm nylon filter paper and washed with 20 mL 20:1 acetone:water, then 20 mL of acetone. The pink solid (879 mg) was then dissolved in H_2O (44 mL) and to this solution was added a solution of KPF_6 (1.05 g in 40 mL of H_2O). The pH of the mixture was raised to 5.5 by the controlled addition of 0.5 M KOH, causing the formation of a pink precipitate. The precipitate was collected on 5 μm nylon filter paper and washed with 80 mL diethylether. The solid was dissolved in 20 mL of MeCN with heating and stirred for 2 h at $60\text{ }^{\circ}\text{C}$. The solution was concentrated to near saturation and vapor diffusion of Et_2O into the MeCN solution at room temperature yielded orange/red crystals suitable for X-ray diffraction (1.36 g, 1.19 mmol, 84%). ^1H NMR (DMF- d_7 , δ): 9.44 (2H, t), 9.20 (2H, d), 9.14 (2H, d), 9.04 (1 H, s), 9.02 (1H, d), 8.96 (2H, d), 8.46 (8H, m), 7.94 (2H, t), 7.90 (2H, t), 3.33 (3H, s), 3.31 (3H, s), 2.87 (3H, s), 2.39 (2H, s). HR-ESI-MS (m/z): [**1** - (H^+ , 3PF_6^-)] $^{2+}$ calcd ($\text{C}_{34}\text{H}_{31}\text{Co}_2\text{N}_7\text{O}_3$) 703.12; found 703.125. Elemental analysis ($\text{C}_{34}\text{H}_{32}\text{Co}_2\text{F}_{18}\text{N}_7\text{O}_3\text{P}_3$): calcd C 35.84, H 2.83, N 8.61; found C 35.69, H 2.65, N 8.70.

Preparation of $[\text{Co}_2(\text{OH})\text{DPEN}(\mu\text{-}1,3\text{-OC}(\text{NH})\text{CH}_3)](\text{PF}_6)_2$ (2**).** The reduction of **1** to **2** was performed in a glovebox under an inert atmosphere of N_2 . **1** (0.300 g, 0.263 mmol) was dissolved in 10 mL of *N,N*-dimethylformamide (DMF) with stirring. An aliquot of lithium triethylborohydride (LiHBEt_3 , superhydride, 0.1 M THF solution, 2.63 mL, 0.263 mmol) was diluted to 5 mL with DMF and added in a slow dropwise manner to the solution of **1**. The orange solution of **1** immediately became a very dark orange, and over the course of 3 d of

stirring at room temperature became a deep green. After 3 d the solvent was removed *in vacuo*. The solid green material was dissolved in minimal MeCN and vapor diffusion of Et₂O into the MeCN solution at room temperature yielded dark green crystals. This material was only ~70% pure by NMR, so the green crystals were washed thoroughly with DCM, which washed away a brown-green impurity, and the resulting green powder was subjected to the same vapor diffusion, yielding dark green crystals clean by NMR and suitable for X-ray diffraction (0.048 g, 0.049 mmol, 19%). It was found that **2** could also be synthesized in higher yield using decamethylcobaltocene as the reductant. **1** (0.205 g, 0.18 mmol) and dimethylformamidium triflate (0.048 mg, 0.216 mmol) were dissolved in 10 mL of DMF with stirring. A THF solution of decamethylcobaltocene (0.119 g, 0.36 mmol, in 5 mL THF) was added dropwise to the stirring solution of **1**. The solution changed from orange to dark green within 5 min, and the reaction solution was left to stir for 24 h to ensure complete reduction of the starting material. Solvent was removed *in vacuo* until 4 mL of DMF remained, and the dark green product was obtained by precipitation with Et₂O. The green powder was stirred in THF to remove the decamethylcobaltocenium byproduct, and the solid green powder was collected and dissolved in minimal MeCN and vapor diffusion of Et₂O into the MeCN solution at room temperature yield dark green crystals (0.065 g, 0.063 mmol, 37 %). (¹H NMR (DMF-d₇, δ): 9.77 (1H, d), 9.54 (1H, d), 9.14 (1H, d), 9.04 (1H, d), 8.72 (1H, d), 8.67 (1H, d), 8.21 (4H, m), 8.10 (2H, dd), 8.04 (2H, q), 7.71 (2H, m), 7.60 (2H, m), 7.26 (1H, m), 7.19 (1H, d), 6.66 (1H, s), 2.82 (6H, d), 2.21 (3H, s). Peaks at 6.66 and 2.21 ppm are assigned to the amide and methyl, respectively, of the bridging acetamidate ligand. Elemental analysis (C₃₄H₃₁Co₂F₁₂N₇O₂P₂): calcd C 41.78, H 3.20, N 10.03; found C 41.86, H 3.34, N 10.32.

Preparation of [Co₂(OH)DPEN(μ-1,3-OC(NH)CH₃)(μ-O₂)](PF₆)₂ (3**).** A solution of **2** in DMF was prepared in an air-free flask in a dinitrogen filled glovebox, and freeze-pump-thawed on a Schlenk line, to remove all gas species, both in the headspace and dissolved in solution. O₂ was allowed into this evacuated flask, and after 2 h the solution color turned from deep green to a lighter orange-brown. The flask was brought back into the glovebox, and solvent was removed *in vacuo*. The solid orange-brown material was dissolved in minimal MeCN and vapor diffusion of Et₂O into the MeCN solution at room temperature yielded orange-brown microcrystalline powder. ¹H NMR (DMF-d₇, δ): 9.43 (2H, t), 9.18 (2H, d), 9.13 (2H, d), 9.02 (1 H, d), 9.01 (1H, s), 8.95 (2H, d), 8.45 (8H, m), 7.94 (2H, t), 7.89 (2H, t), 3.32 (3H, s), 3.30 (3H, s), 2.87 (3H, s), 2.44 (1H, s).

Reaction of **1 with Urea Hydrogen Peroxide.** Solid dicobalt(III,III) compound **1** was dissolved in DMF and added to a DMF solution of 20 equiv urea hydrogen peroxide (UHP), under a N₂ atmosphere in the glovebox. The solution was transferred to an airtight cuvette and immediately placed in a UV-vis spectrophotometer, and scans were taken every 2 min. Over the course of one hour the solution changed color from pink-red to orange, with clear isosbestic points; the spectrum is shown in Figure S6.

A.3. Characterization methods

NMR spectra were recorded at room temperature on a Varian Inova-500 NMR spectrometer, and DOSY NMR were recorded on an Agilent DD2-600 NMR spectrometer at the Harvard University Department of Chemistry and Chemical Biology Laukien-Purcell Instrumentation Center. ^1H NMR spectra were internally referenced to the residual solvent signal ($\delta = 1.94$ for CD_3CN or $\delta = 2.50$ for $\text{DMSO}-d_6$). Mass spectra were recorded on a Bruker micrOTOF-QII LCMS ESI-TOF mass spectrometer in positive ion mode. All spectra were externally calibrated with sodium formate. UV-vis absorption spectra were acquired using a Cary 5000 spectrometer (Agilent).

Magnetic measurements were recorded using a Quantum Design MPMS 7AC SQUID magnetometer. Solid samples were placed in polycarbonate capsules inserted into plastic straws. DC magnetic susceptibility data was collected over the 2–298 K range at a field of 3.5 T. The data was corrected for the diamagnetic contribution of the capsule and straw using an empty capsule. The magnetic susceptibilities of the compounds were adjusted for diamagnetic contributions using the constitutive corrections from Pascal's constants [3]. Data was fit with the PHI software package [4] to the following Hamiltonian:

$$\hat{H} = -J\hat{S}_A \cdot \hat{S}_B + \beta(\hat{S}_A \cdot g_A + \hat{S}_B \cdot g_B) \cdot B \quad (\text{S1})$$

where J is the exchange coupling constant, \hat{S} is the spin angular momentum operator, β is the Bohr magneton of the electron, g is the electron g -factor, and B is the applied field; the subscripts A and B refer to the two spin components that are coupled. This Hamiltonian accounts for both magnetic exchange (first term) and Zeeman splitting (second term). The SQUID data for compound **2** had a curved component at low temperature that was not consistent with a strongly antiferromagnetically coupled compound, but an excellent fit was achieved by fitting the data as 85% antiferromagnetically coupled with 15% paramagnetic impurity.

X-ray photoelectron spectra were recorded using a Thermo Scientific K-Alpha XPS system. All samples were irradiated using a monochromated Al $K\alpha$ X-ray source (1486.6 eV energy and 0.85 eV line width) with a 400 μm spot size [5]. Surface charging was compensated by a low-energy (0–14 eV) electron flood gun. The system was pre-calibrated with Au, Ag, and Cu standards built into the sample stage using an automated routine. Solutions of the sample were drop-cast onto Au foil. High-resolution spectra for the Co 2p region were measured with a step size of 0.1 eV. Samples were calibrated to the C 1s peak at 284.8 eV [6].

A.4. X-ray crystallography

X-ray diffraction data were collected on a Bruker three-circle platform goniometer equipped with an Apex II CCD and an Oxford cryostream cooling device at 100–275 K. Radiation was supplied from a graphite fine focus sealed tube Mo $K\alpha$ (0.71073 Å) source. Crystals were mounted on a glass fiber using Paratone N oil. Data were collected as a series of φ and/or ω

scans. Data were integrated using SAINT and scaled with a multi-scan absorption correction using SADABS [7]. The structures were solved by intrinsic phasing using SHELXT (Apex2 program suite v2014.1) and refined against F² on all data by full matrix least squares with SHELXL-97. All non-hydrogen atoms were refined anisotropically. Hydrogen atoms were placed at idealized positions and refined using a riding model.

A.5. Details for fitting VT ¹H NMR

Variable temperature ¹H NMR for compound **2** was fit to the curvilinear eq S2 (eq 1 in the Main Text) [8,9],

$$\delta \text{ (ppm)} = \delta_{\text{singlet}} + 10^6 \frac{g\beta_e}{g_N\beta_N} \frac{aS(S+1)}{kT} \left[3 + \exp\left(\frac{\Delta E_{T-S}}{RT}\right) \right]^{-1} \quad (\text{S2})$$

where g and g_N are the electronic and nuclear g -values, respectively, β_e and β_N are the Bohr and nuclear magnetons, respectively, a is the isotropic hyperfine coupling constant, S is the spin of the system ($S = 1$ for a triplet), k is the Boltzmann constant, and R is the gas constant. The measured chemical shifts were fit to equation S3, with an R^2 value of 0.991:

$$\delta(\text{ppm}) = A + 10^6 \frac{B}{T} \left[3 + \exp\left(\frac{C}{T}\right) \right]^{-1} \quad (\text{S3})$$

where $A = \delta_{\text{singlet}}$, $B = \frac{g\beta_e}{g_N\beta_N} \frac{aS(S+1)}{k}$, and $C = \frac{\Delta E_{T-S}}{R}$.

The following values were obtained from the fit, with their standard errors in parentheses:

$$A = 6.92386 \text{ (0.10329)}$$

$$B = 0.00694 \text{ (0.00285)}$$

$$C = 1324.5173 \text{ (245.51426)}$$

Using the above relations, the parameters a and ΔE_{T-S} were determined as follows:

$$B = 0.00694 = \frac{2.0023(9.2741 \times 10^{-21} \text{ erg G}^{-1})}{5.58569(5.0508 \times 10^{-24} \text{ erg G}^{-1})} \frac{2a}{1.3807 \times 10^{-16} \text{ erg K}^{-1}}$$

$$a = 7.27889 \times 10^{-22} \text{ erg}$$

$$C = 1324.5174 = \frac{\Delta E_{T-S}}{R} = \frac{\Delta E_{T-S}}{8.311446 \times 10^7 \text{ erg K}^{-1} \text{ mol}^{-1}}$$

$$\Delta E_{T-S} = 1.1009 \times 10^{11} \text{ erg mol}^{-1}$$

To convert to a in erg to G:

$$a \text{ G} = \frac{a \text{ erg}}{g\beta_e} = \frac{7.27889 \times 10^{-22} \text{ erg}}{2.0023(9.2741 \times 10^{-21} \text{ erg G}^{-1})} = 0.0392 \text{ G}$$

To convert ΔE_{T-S} in erg mol^{-1} to kJ mol^{-1} :

$$\Delta E_{T-S} = 1.1009 \times 10^{11} \text{ erg mol}^{-1} \left(\frac{10^{-7} \text{ J}}{1 \text{ erg}} \right) \left(\frac{1 \text{ kJ}}{10^3 \text{ J}} \right) = 11.01 \text{ kJ mol}^{-1}$$

A.6. Computational details

Density functional theory (DFT) calculations were performed with the hybrid functional Becke-3 parameter exchange functional [10–12] and the Lee–Yang–Parr non-local correlation functional (B3LYP) [13] as implemented in the Gaussian 09, Revision D.01 software package [14]. For light atoms (H, C, N, O, and F), a polarized split-valence triple- ζ basis set that includes p functions on hydrogen atoms and d functions on other atoms (*i.e.* the 6-311G(d,p) or 6-311G** basis set) was used. A Dirac-Fock [15,16] relativistic effective core potential (*i.e.*, MDF10) was used for Co. The system was treated as a spin-restricted Co(III,III) singlet state. All calculations were performed with a polarizable continuum (PCM) solvation model in acetonitrile using a polarizable conductor calculation model (CPCM) [17,18]. All geometries were confirmed as local minima structures by calculating the Hessian matrix and ensuring that no imaginary eigenvalues were present.

B. Figures

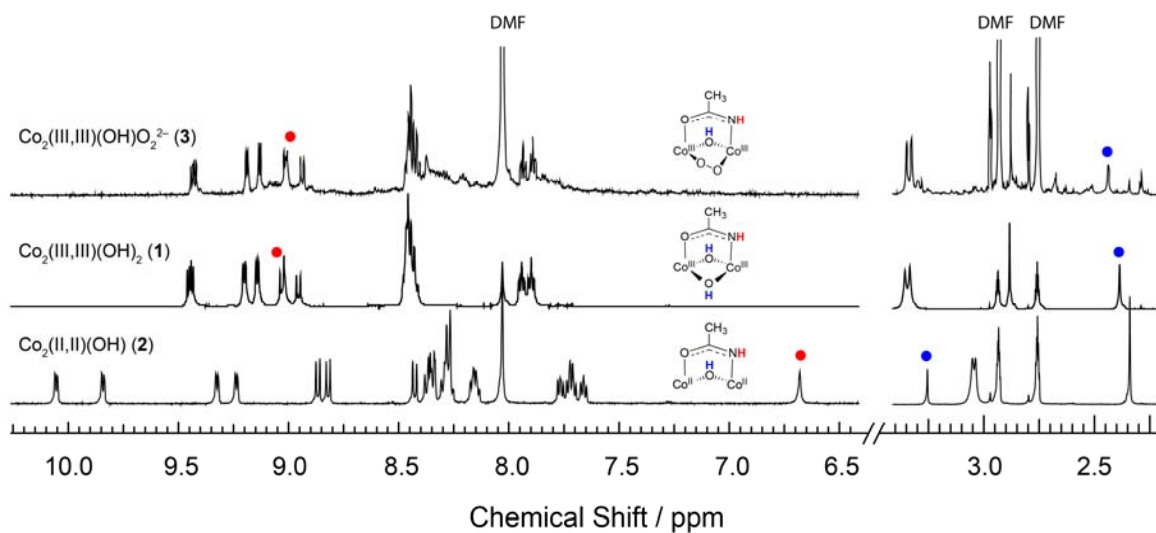


Figure S1. Nuclear magnetic resonance (NMR) spectra of compounds **1**, **2** and **3** in $\text{DMF-}d_7$. Peaks assigned to the acetamidate N-H proton are marked with a red circle, and O-H protons are marked with a blue circle. The NMRs of **1** and **3** are similar, due to the similar electronic structure of both compounds. Slight differences are seen in the N-H and O-H shifts. Chemical shifts and peak integrations are detailed in A.2. Synthesis described on pages S3-S5.

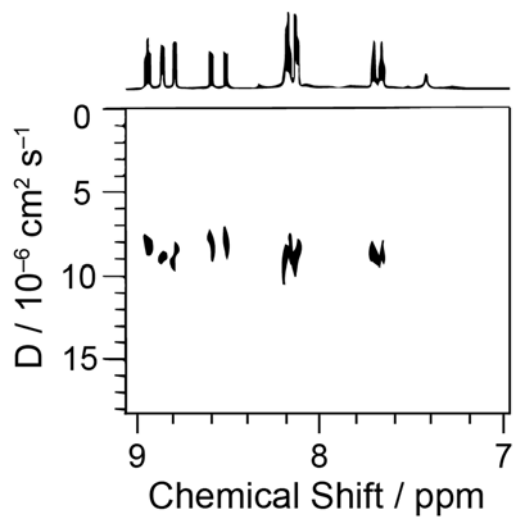


Figure S2. 2-D DOSY NMR spectroscopy of a 9 mM solution of **1** in MeCN- d_3 . The values of the diffusion coefficient (D , y-axis) obtained for each proton chemical shift are averaged to yield $D = 8.5 \times 10^{-6} \text{ cm}^2 \text{ s}^{-1}$.

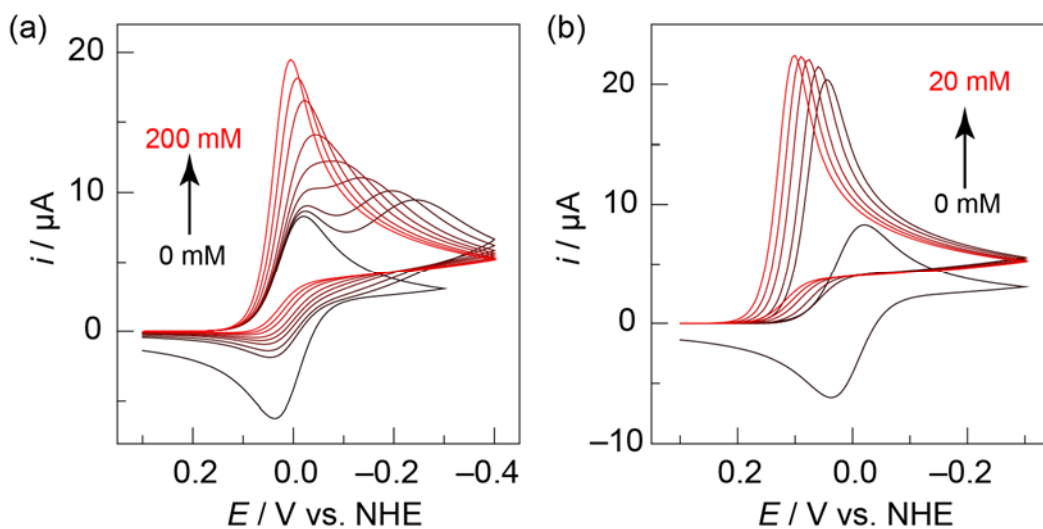


Figure S3. Simulations of an E(EC) mechanism using DigiElch and the parameters of **1** (0.5 mM) in MeCN and 0.1 M $n\text{-Bu}_4\text{NPF}_6$ at a scan rate of 0.1 V s^{-1} . Titration of acid: 0 (—) to 200 (—) mM in (a) and 0 (—) to 20 (—) mM in (b). The parameters concerning the second electron–proton transfer are unknown, so the simulation was performed by fixing the kinetic constant of this electron transfer, and using a different standard potential in (a) and (b), as the standard potential of a concerted proton–electron transfer depends on the $\text{p}K_{\text{a}}$ of the acid: (a) simulates a weak acid and (b) simulates a strong acid, and the simulated CVs match the waveforms of the experimental CVs in AcOH and TFA, respectively, indicating that E(EC) is a viable mechanism.

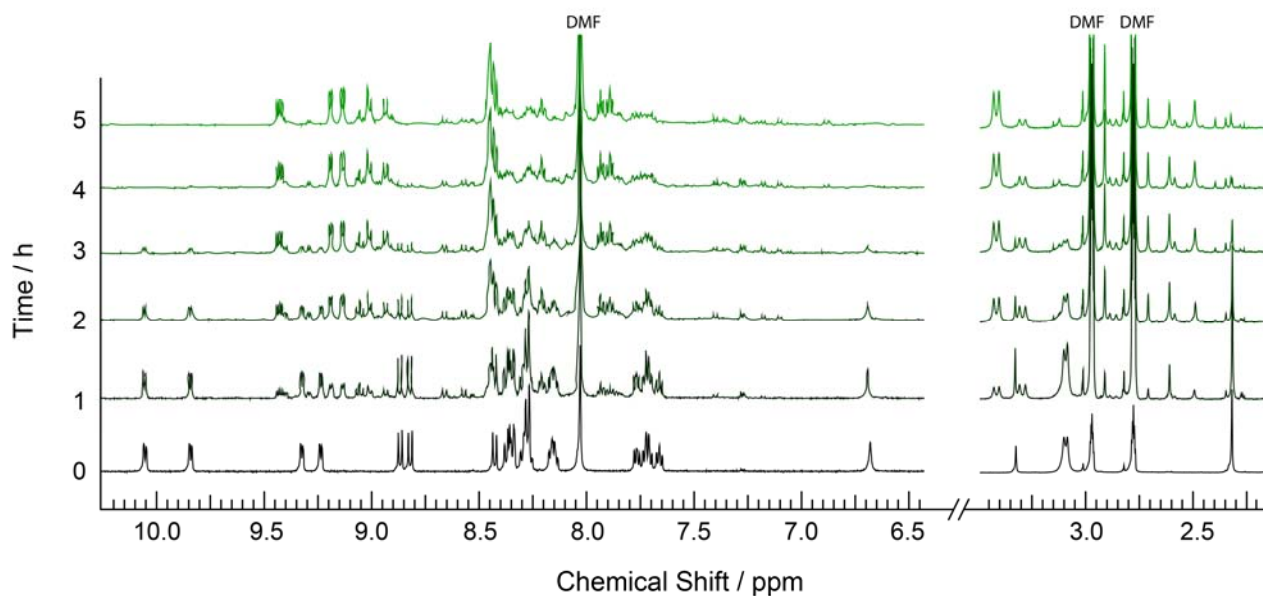


Figure S4. O₂ binding to **2** in DMF-*d*₇. The starting material **2** (—) converts to compound **3** (—) over the span of 5 h. Spectra were taken every hour.

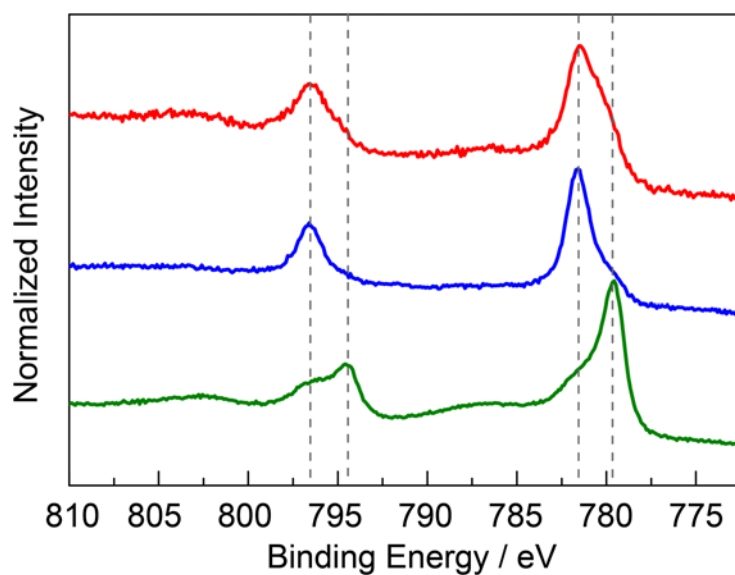


Figure S5. Co 2p region of the XPS spectrum collected for compound **3** (■). Spectra of **1** (■) and **2** (■) are provided as authentic Co₂(III,III) and Co₂(II,II) samples, respectively, in the same ligand environment as **3**, the compound of interest. Dotted gray lines are added to guide the eye to the binding energies of Co(II) and Co(III) species.

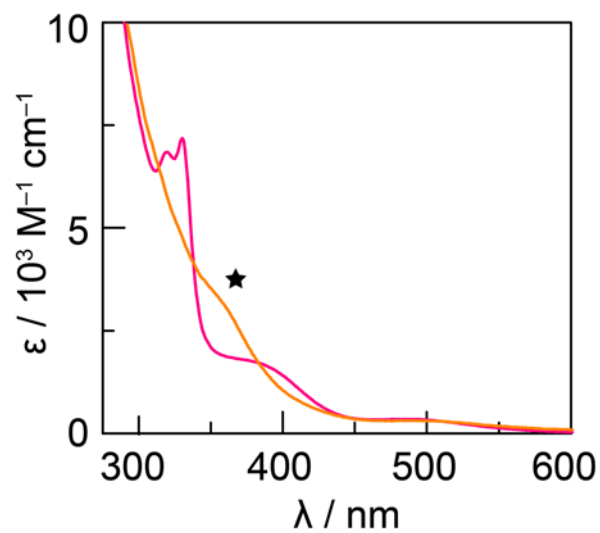


Figure S6. (a) Reaction of **1** (red) with urea hydrogen peroxide in DMF over the course of 1 h to produce a spectrum (orange) that is similar to **3**, as shown in Figure 7 of the text. The characteristic product band at 360 nm is marked with a star.

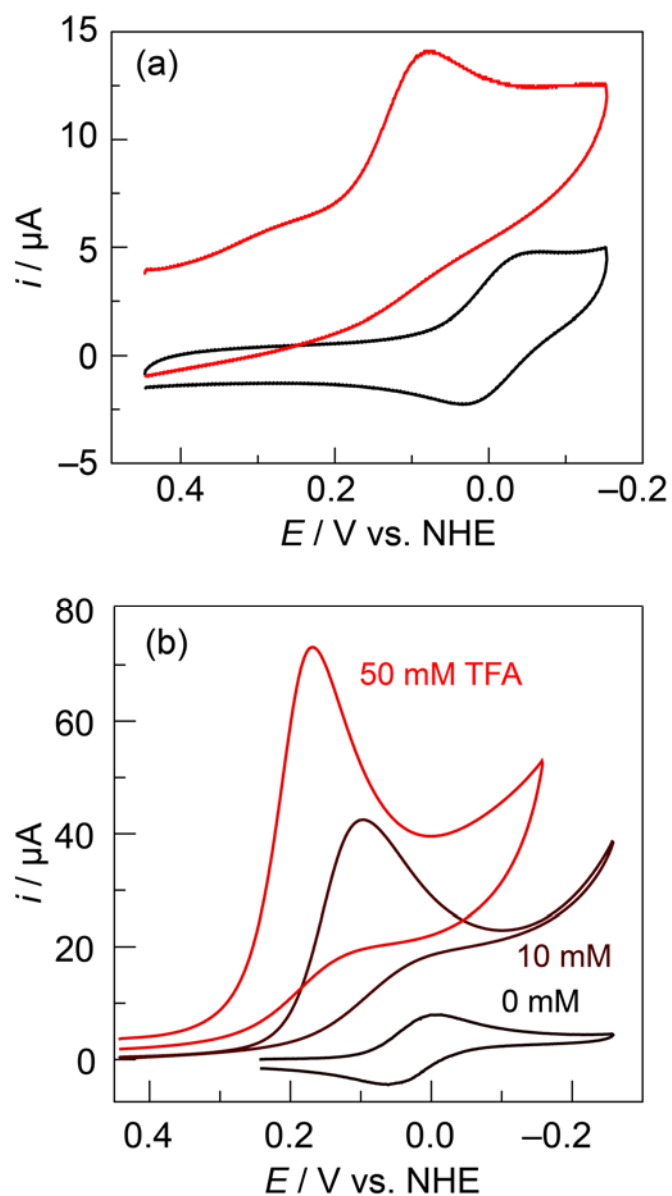


Figure S7. (a) Cyclic voltammogram (CV) of **3** (1 mM) in MeCN and 0.1 M *n*-Bu₄NPF₆ under N₂ and in the presence of increasing concentrations of TFA. (b) CV of **1** (0.5 mM) in MeCN and 0.1 M *n*-Bu₄NPF₆ under 8.1 mM O₂ and in the presence of increasing concentrations of TFA. The reversible reduction exhibited by **1** in the absence of O₂ and TFA is included for comparison (black trace).

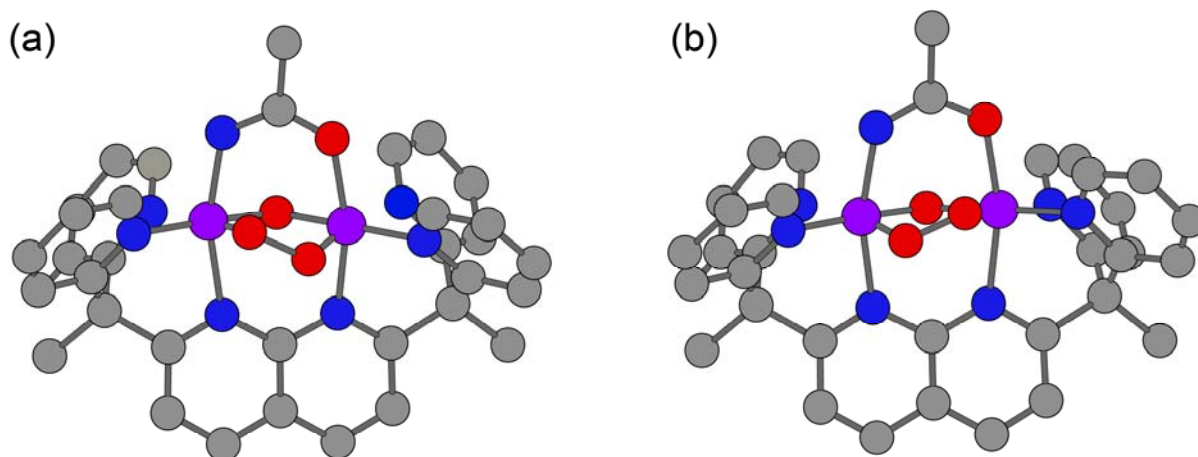


Figure S8. DFT calculated geometries for **3**. Both (a) and (b) represent viable stable geometries for the O₂ moiety. The geometry in (b) is more stable than that in (a) by 2.94 kJ/mol

References

1. T. C. Davenport and T. D. Tilley, *Angew. Chem. Int. Ed.*, 2011, **50**, 12205.
2. E. A. Ünal, D. Wiedemann, J. Seiffert, J. P. Boyd and A. Grohmann, *Tet. Lett.*, 2012, **3**, 54.
3. G. A. Bain and J. F. Berry, *J. Chem. Ed.*, 2008, **85**, 532.
4. N. F. Chilton, R. P. Anderson, L. D. Turner, A. Soncini and K. S. Murray, *J. Comput. Chem.* **2013**, *34*, 1164.
5. J. F. Watts and J. Wolstenholme, *An Introduction to Surface Analysis by XPS and AES*, John Wiley and Sons: Chichester, UK, 2003.
6. T. L. Barr and S. J. Seal, *J. Vac. Sci. Technol. A*, 1995, **13**, 1239.
7. Bruker AXS (2009). Apex II. Bruker AXS, Madison, Wisconsin.
8. B. Le Guennic, T. Floyd, B. R. Galan, J. Autschbach and J. B. Keister, *Inorg. Chem.*, 2009, **48**, 5504.
9. C. M. Lemon, M. Huynh, A. G. Maher, B. L. Anderson, E. D. Bloch, D. C. Powers and D. G. Nocera, *Angew. Chem. Int. Ed.*, 2016, **55**, 2176.
10. A. D. Becke, *Phys. Rev. A*, 1988, **38**, 3098.
11. A. D. Becke, *J. Chem. Phys.*, 1993, **98**, 1372.
12. A. D. Becke, *J. Chem. Phys.*, 1993, **98**, 5648.
13. C. Lee, W. Yang and R. G. Parr, *Phys. Rev. B*, 1988, **37**, 785.
14. M. J. Frisch, G. W. Trucks, H. B. Schlegel, G. E. Scuseria, M. A. Robb, J. R. Cheeseman, G. Scalmani, V. Barone, B. Mennucci, G. A. Petersson, H. Nakatsuji, M. Caricato, X. Li, H. P. Hratchian, A. F. Izmaylov, J. Bloino, G. Zheng, J. L. Sonnenberg, M. Hada, M. Ehara, K. Toyota, R. Fukuda, J. Hasegawa, M. Ishida, T. Nakajima, Y. Honda, O. Kitao, H. Nakai, T. Vreven, J. A. Montgomery, Jr., J. E. Peralta, F. Ogliaro, M. Bearpark, J. J. Heyd, E. Brothers, K. N. Kudin, V. N. Staroverov, R. Kobayashi, J. Normand, K. Raghavachari, A. Rendell, J. C. Burant, S. S. Iyengar, J. Tomasi, M. Cossi, N. Rega, J. M. Millam, M. Klene, J. E. Knox, J. B. Cross, V. Bakken, C. Adamo, J. Jaramillo, R. Gomperts, R. E. Stratmann, O. Yazyev, A. J. Austin, R. Cammi, C. Pomelli, J. W. Ochterski, R. L. Martin, K. Morokuma, V. G. Zakrzewski, G. A. Voth, P. Salvador, J. J. Dannenberg, S. Dapprich, A. D. Daniels, Ö. Farkas, J. B. Foresman, J. V. Ortiz, J. Cioslowski, D. J. Fox, *Gaussian 09*, Revision D.01; Gaussian, Inc., Wallingford, CT, 2009.
15. Y. S. Lee, W. C. Ermler and K. S. Pitzer, *J. Chem. Phys.*, 1977, **67**, 5861.
16. B. Metz, H. Stoll and M. Dolg, *J. Chem. Phys.*, 2000, **113**, 2563.
17. V. Barone and M. Cossi, *J. Phys. Chem. A*, 1998, **102**, 1995.
18. M. Cossi, N. Rega, G. Scalmani and V. Barone, *J. Comput. Chem.*, 2003, **24**, 669.